Structural characterization and biological evaluation of a new O-acetyl-1,4-linked-β-d-mannan possessed potential application in hydrophilic polymer materials from Dendrobium devonianum

Tao-Bin He, Yan-Ping Huang, Xuan-Jun Wang, Jun Sheng, Jiang-Miao Hu

PII: S0141-8130(22)01072-8

DOI: https://doi.org/10.1016/j.ijbiomac.2022.05.098

Reference: BIOMAC 21096

To appear in: *International Journal of Biological Macromolecules*

Received date: 22 December 2021

Revised date: 5 May 2022

Accepted date: 12 May 2022

Please cite this article as: T.-B. He, Y.-P. Huang, X.-J. Wang, et al., Structural characterization and biological evaluation of a new O-acetyl-1,4-linked-β-d-mannan possessed potential application in hydrophilic polymer materials from Dendrobium devonianum, *International Journal of Biological Macromolecules* (2021), https://doi.org/10.1016/j.ijbiomac.2022.05.098

Structural characterization and biological evaluation of a new *O*-acetyl-1,4-linked-*β*-D-mannan possessed potential application in hydrophilic polymer materials from *Dendrobium devonianum*

Tao-Bin He[a,1], Yan-Ping Huang[b, c,1], Xuan-Jun Wang[b,c,*], Jun Sheng[b,c,*], Jiang-Miao Hu[a,d,*]

[a]State Key Laboratory of Phytochemistry and Plant Resources in West China, Kunming Institute of Botany, Chinese Academy of Sciences, Kunming 650201, Yunnan, People's Republic of China

[b]College of Science, Yunna Agricultural University, KunMing, Yunnan 650000, China

[c]Key Laboratory of Pu-er Tea Science, Ministry of Education, Yunnan Agricultural University, Kunming 650201, China

[d]Bio-Innovation Center of DR PLANT, Kunming Institute of Botany, Chinese Academy of Sciences, Kunming, 650201, Yunnan, People's Republic of China

*** Corresponding Author**

Corresponding author.Tel.: +86-871-65223264

E-mail address: X.J. Wang: xuanjunwang@qq.com; J. Sheng: shengjunpuer@163.com or J.M. Hu: hujiangmiao@mail.kib.ac.cn

[1]T. H. and Y. H. contributed equally to this work.

ABSTRACT

To explore the active polysaccharides from *Dendrobium devonianum*, a novel *O*-acetylmannan (DDP-1) with molecular weight of 117 kDa was isolated from *D. devonianum*. The chemical and instrumental analysis indicated that the DDP-1 was a homopolysaccharide containing a backbone chain composed of →4)-*β*-D-Man*p*-(1→ (71.4%) residue with internal →4)-2-*O*-acetyl-*β*-D-Manp-(1→ (14.2%), →4)-3-*O*-acetyl-*β*-D-Man*p*-(1→ (7.1%), and non-reducing end *β*-D-Man*p*-(1→ (7.3%) residues. Anticancer assay in *vitro* revealed that DDP-1 had anticancer activity against the growth of HepG2 and MCF-7 cancer cells. Moreover, cytokine secretion assays also presented that DDP-1 can promote cytokine production of TNF-*α* and IL-6 in THP-1 macrophage stimulated by PMA. Finally, the effects of isolation and purification on the microstructure of DDP-1 was studied by scanning electron microscope. The morphological features of DDP-1 indicated that DDP-1 hold high potential application in hydrophilic polymer materials.

KEYWORDS: *Dendrobium devonianum*; Polysaccharide; Structural elucidation; Morphological feature; Immunomodulation; Anticancer;

1. Introduction

Dendrobium devonianum, belonging to the *Dendrobium* (Orchidaceae) genus, is a kind of precious medicinal plant well known by Chinese people for more than hundred years and an herbaceous perennial plant (Fig. 1), mainly distributed in Yunnan, Guangxi, Sichuan, and Guizhou Provinces of China [1]. Its stem has been used as a tonic herb in traditional medicine, such as treatment of hepatitis, asthma and immunological disorders [2, 3]. To date, plenty of polysaccharides isolated from *Dendrobium* genus were reported to have potent bioactivities such as antioxidant, anti-hyperglycemic, immuno-stimulating, antiglycation, and antitumor activities [4-8]. In our previous study, a large amount of crude polysaccharide 15% (w/w) was extracted from *D. officinale* and which presented significant immune-modulating and hypoglycemic activity properties [9-11]. To investigate whether polysaccharides play a leading role in *D. devonianum*, crude polysaccharides were extracted from *D. devonianum*. Compared with *D. officinale* polysaccharides, the fine structural characterization of *D. devonianum* polysaccharides was still unclear although a few studies on *D. devonianum* polysaccharides were reported [1, 12, 13]. Therefore, the crude polysaccharides were purified through gel filtration chromatography and anion-exchange chromatography as well as its structural feature was determined by high performance liquid chromatography (HPLC), gas chromatography (GC), fourier transform-infrared (FT-IR) spectroscopy and nuclear magnetic resonance (NMR) in this study. So far, the immunomolulatory activities of *D. devonianum* is the widely acknowleged function in practice among all its biological activities [12, 14]. Thus, the immunoregulatory and antineoplastic activites of purified polysaccharide (DDP-1) was performed in this study. The results showed that DDP-1 presented remarkable immune-enhancing properties and antitumor activity *in vitro*. Furthermore, the biological and chemical properties of polysaccharides are closely correlated with their surface morphology and chain conformation,

which was always affected by different manufacturing processes [15, 16]. To explore the effects of isolation and purification on microstructural feature, the surface morphological features of all samples were observed by scanning electron microscope (SEM). The results suggested that DDP-1 hold high potential application in functional materials.

Fig. 1. *Dendrobium devonianum* cultivated in Longling county

2. Experimental section

2.1. Materials and regents

The stems of *D. devonianum* were collected in Longling county (Yunnan province, P.R. China) in June 2014. It was authenticated by Dr Zhikun Wu of Guizhou University of Traditional Chinese Medicine, and voucher specimens (KIB2016100901) were deposited at the herbarium of Kunming Institute of Botany, Chinese Academy of Sciences. Both DEAE-cellulose-52 (DE52) and Sepharose 6B were purchased from Whatman Co. Dextrans

of different molecular weights were bought from Sigma Co. All other reagents in this research were of grade AR.

2.2. Extraction and purification of DDP-1

Polysaccharides were extracted by the method of our prvious study [11]. Briefly, the dried stems of *D. devonianum* were crushed into powder (218 g) which was pre-treatment twice for 24 h in a soxhlet system with petroleum ether and subsequently for another 4 h with EtOH in order to remove some fat-soluble contents and pigments. The extracts were filtrated through multi-layer gauze and the residue was further extracted three times with 4 L hot deionized water (97 °C). The combined extracts were filtrated and concentrated to a certain volume (about 5 L) with a rotary evaporator under 60 °C, subsequently mixed with ethanol (1:4 v/v) at 4 °C for 24 h to precipitate polysaccharides. After precipitation, the sample was centrifuged at a speed of 4000 rpm for 30 min. The precipitation was dissolved in moderate amounts of distilled water and deproteinized five times by the Sevag method [17]. The polysaccharide solution was further dialyzed against tap water (molecular weight cutoff of 7000 Da) for a night and subsequently for another 2 days with distilled water to yield non-dialysate (molecular weight>7000 Da). The non-dialysate was lyophilized to give the crude polysaccharide (DDP, 41.32 g, 19%). After dryness, the crude polysaccharides (200 mg) were dissolved in 100 mL of distilled water, centrifuged at a speed of 4500 rpm for 30min and then loaded into DEAE52 column (60 × 2.6 cm). Distilled water and NaCl step gradient (0.1, 0.5, 1 M) were used as elution and a total of 40 mL of eluent each was collected. The collection was freeze-dried to ford dried product (140 mg, 70%) and the dried product (50 mg) was further purified on a Sepharose 6B gel column (200 × 2.0 cm) with distilled water to get the purified polysaccharide (DDP-1, 42 mg, 84%). All fractions were monitored with phenol–H_2SO_4 method [18] and high-performance gel-permeation chromatography (HPGPC) equipped with column of Agilent PL aqua gel-OH column (serial

No.0001023217-11) as well as ultraviolet spectrophotometry (UV). The following programs of HPLC-GPC was adopted: 0.01 mol/mL

PBS (Phosphate Buffered Saline; PH: 7.2–7.4) was used as eluent at flow rate of 0.8 mL/min; injection volume was 20 μL.

2.3. Structural characteristics of DDP-1

2.3.1. Molecular weight analysis

The molecular weight of polysaccharide was determined by numerous analytical methods [19]. In this study, the molecular mass of DDP-1 was estimated by high performance gel-permeation chromatography (HPGPC) equipped with column of Agilent PL aqua gel-OH column (serial No.0001023217-11), eluted with 0.01 mol/L PBS (Phosphate Buffered Saline, PH: 7.2-7.4) at a flow rate of 0.8 mL/min. Injection volume was 20 μL. Both the column and detector temperatures were 35 °C. The following dextrans were used as standard sample: 31425 (Sigma, M_W: 670 kD), 31424 (Sigma, M_W: 410 kD), 31422 (Sigma, M_W: 150 kD), 31420 (Sigma, M_W: 50 kD), 31418 (Sigma, M_W: 12 kD), respectively.

2.3.2. Monosaccharide composition analysis

The DDP-1 (11.2 mg) were hydrolyzed in 2 M trifluoroacetic acid (15 mL) at 100 °C for 2 h [20]. After reduction with sodium borohydride, acetic acid was respectively added into the sample (hydrolysate, glucose, mannose, rhamnose and inositol) to remove extra borohydride and dried by rotary evaporation combined with vacuum-freeze dryer. These samples then were acetylated with 1:1 pyridine–Ac_2O (100 °C, 3 h), the acetylated derivatives were extracted with 20 mL of methylene chloride. The methylene chloride layer was treated with anhydrous sodium sulfate, and then was filtered through 0.22 μm of nylon membrane, after which the acetylated derivatives were analyzed by gas chromatography system equipped with a HP-5 capillary column (30 m × 0.320 mm × 0.25 μm, Serial NO: USB608846H) and a flame ionization detector. The column temperature programmed from 140 °C held for 1

min, increasing to 200 °C with a rate of 2 °C/min, then to 280 °C at 5 °C /min. The injector and detector temperatures were set to 250 °C and 280 °C, respectively. Nitrogen carrier gas was at 1 mL/min.

2.3.3. Methylation Analysis

A solution of 5 mg of dry DDP-1 dissolved in 2 mL of DMSO was permethylated by adding 50 mg of finely powdered NaOH. The mixture was then treated with an ultrasonic cleaner. After incubation for 2 h at room temperature, 1 mL of methyl iodide was added for DDP-1 methylation. The sample was kept in darkness for 1 h before distilled water was used to decompose the remaining methyl iodide. The methylated polysaccharides were extracted with 4 mL of chloroform and dried at low pressure on a rotary evaporator. After hydrolysis with 10 mL of 2 M trifluoracetic acid, the hydrolysates were dissolved in 3 mL of NaOH aqueous solution. A total of 20 mg of $NaBH_4$ were added to reduce the hemiacetal group. After incubation at 25 °C for 2 h, the sample was dried under low pressure, and then acetylated by adding 2 mL of acetic anhydride and 2 mL of pyridine. The reaction was kept at 100 °C for 1 h. A total of 2 mL of distilled water were used to decompose the remained acetic anhydride. The acetylated derivatives were extracted with 4 mL of methylene chloride. The methylene chloride layer was treated with anhydrous sodium sulfate, and then was filtered through 0.22 μm of nylon membrane, after which the acetylated derivatives were analyzed by gas chromatography-mass spectrometer equipped with a HP-5 capillary column (30 m × 0.320 mm × 0.25 μm, Serial NO: USB608846H) and a mass spectrometry detector. The column temperature programmed from 140 °C held for 1 min, increasing to 200 °C with a rate of 2 °C /min, then to 280 °C at 5 °C/min. The injector and detector temperatures were set to 250 °C and 280 °C, respectively. Nitrogen carrier gas was at 1 mL/min. The mass spectrometer was operated in electron impact (EI) mode at 70 eV and scan rage of 35–500

amu. The temperatures were 150 °C for the MS Quad, 230 °C for the MS Source, and 250 °C for the transfer line.

2.3.4. Infrared spectral analysis

The dried DDP-1 (1 mg) was ground with KBr (100 mg) powder and then pressed into pellets for IR (Tensor27) measurement in the frequency range of 4000–500 cm^{-1}.

2.3.5. NMR spectroscopy

DDP-1 (10 mg) was dissolved in 99.9% D_2O (Euriso-Top) and deuterium-exchanged by lyophilizing three times. Then the freeze-dried sample was dissolved in 99.9% D_2O in an NMR tube (5 mm diameter). NMR spectra were recorded at Cona Bruker AvanceTM DXM (800 MHz) single-channel NMR spectrometer equipped with an inverse 5-mm triple-resonance probe. Chemical shifts are reported in ppm and Data processing was performed by MestReNova software.

2.3.6. Molecular surface morphology analysis

The surface morphological feature of polysaccharides freeze-dried were recorded using scanning electron microscopy (SEM, CARL ZEISS and QUORUM, Sigma300, Germany). Samples were dispersed onto an aluminum stub and gold coated with an ion sputter coater. An acceleration voltage of 10 kV was applied.

2.4. Biological evaluation

2.4.1. Assessment of anti-tumor activity

The anti-tumor activity of DDP-1 was estimated by MTT assay. Human hepatoma cell lines (HepG2) and human breast cancer cell lines (MCF-7) were cultured in DMEM/HIGH GLUCOSE (1:1, HyClone) medium, respectively. Each cell line was plated in 200 μL medium at the appropriate seeding density (5000 cells/well) into 96 well microtitre plates. Then DDP-1 was added with a concentration gradient (25, 50, 75, 100, 150, 300 μg/mL). Control group without DDP-1 was conducted in parallel. A total of 20 μL of MTT (5

mg/mL) solution was added into each well 48 h later. After incubation for 4 h, 150 μL of dimethyl sulfoxide were added into each well removed the MTT medium. The light absorption at 560 nm was determined by microplate reader. The inhibiton ratio (%) was calculated according to the following formula: $A=(1-A_E/A_C) \times 100\%$ where A is the tumor cell growth repression rate; A_E is the optical density of experimental group; and A_C is the optical density of control group.

2.4.2. Evaluation of immunostimulating effects

THP-1 cells (1×10^6 cells/mL) were plated onto a sixty millimetres plate in a total volume of 5 mL culture medium. The cells were induced into the mature macrophage-like state by treating THP-1 monocytes for 48 h with PMA. Subsequently, the cells were cultured in improved RPMI 1640 (Gibco, HyClone) without any fetal bovine serum or penicillin/streptomycin for 20 h to ensure that they reverted to a resting phenotype before the cells were treated with RPMI 1640 (negative control), lipopolysaccharide (LPS, 50 ng/mL, positive control), or DDP-1 in various concentrations (25, 50, 75, 100, 150, 300 μg/mL, respectively). The cytokine production stimulated in cells was determined by the enzyme-linked immunosorbent assay (ELISA) procedure according to the protocol provided by the supplier (R&D Systems, Minneapolis, MN, USA). Triplicate measurements were obtained for each sample.

2.5. Statistical analysis

The results in this study were from three independent experiments and presented as the means ± standard deviations (SD). Statistical analysis was performed by a one-way Analysis of Variance (ANOVA) in Statistical Prism 6 software. * $P < 0.5$, ** $P < 0.01$, *** $P < 0.001$ vs negative control.

3. Results and discussion

3.1. Extraction and purification of DDP-1

After hot water extraction and ethanol precipitation, the crude polysaccharide was got from *D. devonianum*, which mainly contains three peaks by HPLC analysis (Fig. 2A). Sevag method [17], a common and wide method, was adopted to remove protein and the result of HPLC analysis showed deproteined polysaccharide contains two peaks (Fig. 2B). Furthermore, to obtain homogeneous polysaccharides from *D. devonianum*, dialysis bag (molecular weight cutoff: 7000 Da) was used to remove small molecules (Fig. 2C). Finally, the dried non-dialysate was further purified on anion exchange chromatogram (DEAE52). The first peak was the leading polysaccharide fraction with a trace of fraction eluted by 1 M NaCl (Fig. 2D). After dried, a total of 2 mL of the fraction (2 mg/mL) was further loaded on a Sepharose 6B column to give a pure fraction (DDP-1), demonstrated in Fig. 2E. In addition, the HPLC-GPC analysis also exhibited a single and symmetrical peak as well as UV spectrum indicated no absorbance near 260 and 280 nm (Fig. 2F and G), which illustrated its homogeneity based on the distribution of molecular weight. The productivity of DDP-1 was 11.2% based on the mass of dried plant material.

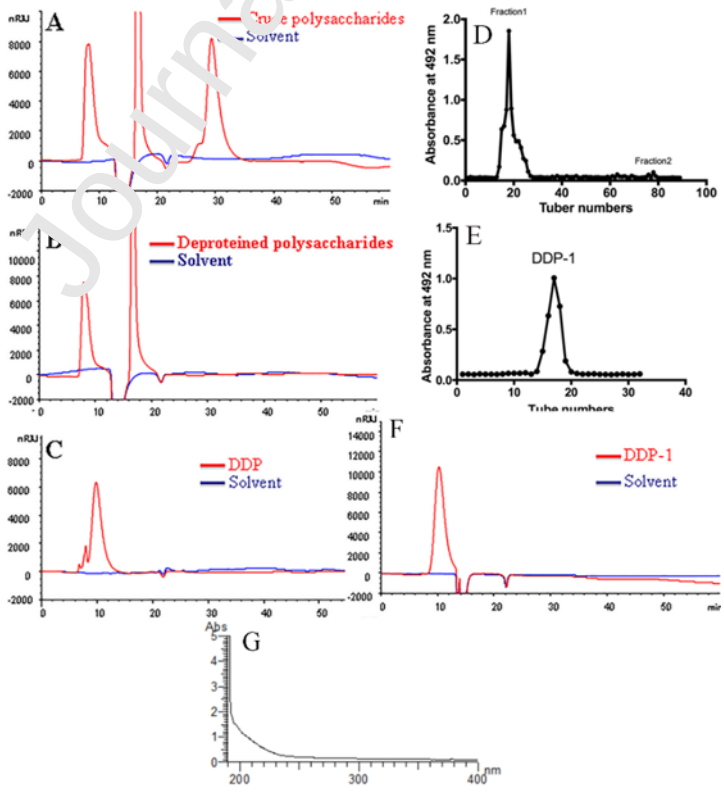

Fig. 2. Extraction and purification of DDP-1: (**A**) Ethanol precipitation, (**B**) Deproteined polysaccharide (**C**) Membrane filtration. (**D**) Purified polysaccharide by DEAE52, (**E**) Purified polysaccharide by gel filtration, (**F**) HPLC profile of DDP-1. (**G**) UV spectrum of DDP-1.

3.2. Molecular weight and monosaccharide composition

The molecular mass of DDP-1 was 1.17 × 10^5 Da based on comparison with a standard plot of dextrans by HPGPC analysis (Fig. 3A) which was different from the molecular mass of *D. devonianum* polysaccharides reported by other researchers [1, 12, 13]. To investigate the monosaccharide composition of DDP-1, DDP-1 was totally hydrolyzed with 2 M TFA into individual monosaccharides and then derivatized into alditol acetates for gas chromatography analysis. The results demonstrated DDP-1 was a homopolysaccharide composed of mannose, namely mannan (Fig. 3B). Compared with other species, the monosaccharide composition of DDP-1 was single although other *Dendrobium* polysaccharides also mainly contained mannose [21].

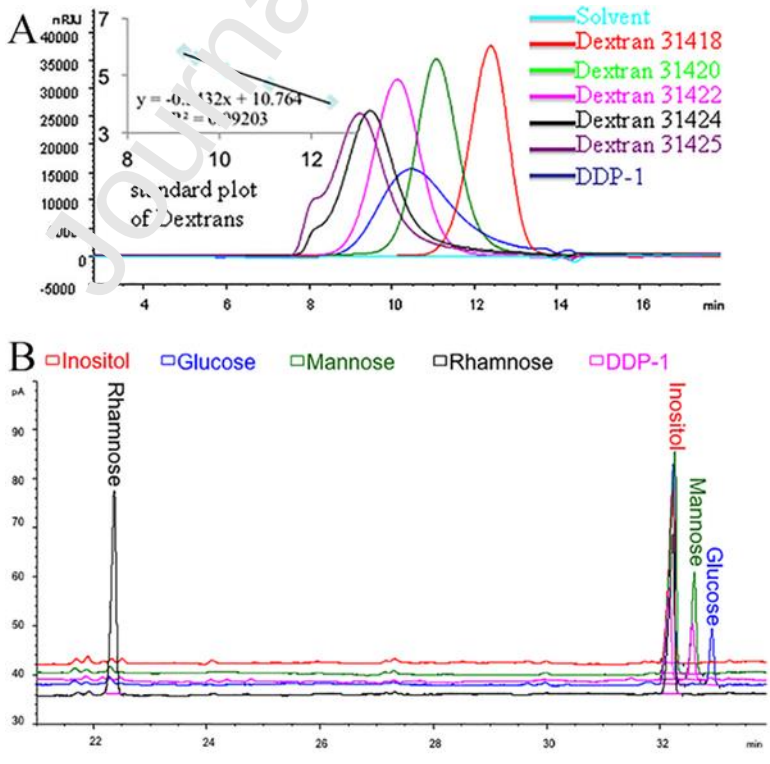

Fig. 3. (**A**) Molecular weight measurement of DDP-1, (**B**) Gas chromatogram of monosaccharide composition of DDP-1.

3.3. Methylation analysis of DDP-1

To date, the methylation analysis of *D. devonianum* polysaccharide was not reported [1, 12, 13]. In order to identify the glycosidic linkage, methylation and acetylation was taken to derivatize DDP-1. The result demonstrated that DDP-1 was composed of residues Man*p*-(1→ and→4)-Man*p*-(1→ based on the retention time and mass spectra (Table 1 and Fig. S1–5). The relative content of each peak was determined as 1:26 by the normalization method of peak area. This result showed that the structure of DDP-1 was different from other *Dendrobium* species polysaccharides based on the ratio of the residues Man*p*-(1→ and→4)-Man*p*-(1→ [21].

Table 1. GC-MS analysis of methylated of DDP-1

Linkage type	Retention time	Major mass fragments (m/z)	Molar ratio
Man*p*-(1→	14.17	43, 71, 87, 101, 117, 129, 145, 161, 205	1
→4)-Man*p*-(1→	17.82	43, 87, 101117, 143, 161, 233	26

3.4. Fine structural elucidation of DDP-1

3.4.1. FT-IR and 1D NMR analysis of DDP-1

To further identify the structural characteristics of DDP-1, FTIR spectrum and NMR spectra were adopted (Fig. 4A–C and S6–8). According to the infrared (IR) spectrum of DDP-1, a broad stretching peak at 3405 cm^{-1} indicated the presence of hydroxyl group. Furthermore, the signals at 2924, 2890 cm^{-1} are due to C-H stretching and the signal at 1382 cm^{-1} from bending vibration (Fig. 4A and S6). The signals at δ 2.09–2.10 ppm in ^{1}H NMR (Fig. 4B and S7) and carbon signals at δ 19.8–20.0 and δ 172.4 ppm from the ^{13}C NMR spectra (Fig. 4C

and S8) indicated the existence of acetyl group, which was further confirmed by and absorption at 1632 cm^{-1} from IR spectra [22]. The peaks of 815, 871, 895 cm^{-1} in IR spectra as well as no any signals at 82–88 ppm in ^{13}C NMR spectra suggested that mannose was in pyranose sugar forms. The fine structure of DDP-1 was further elucidated by 2D NMR spectra.

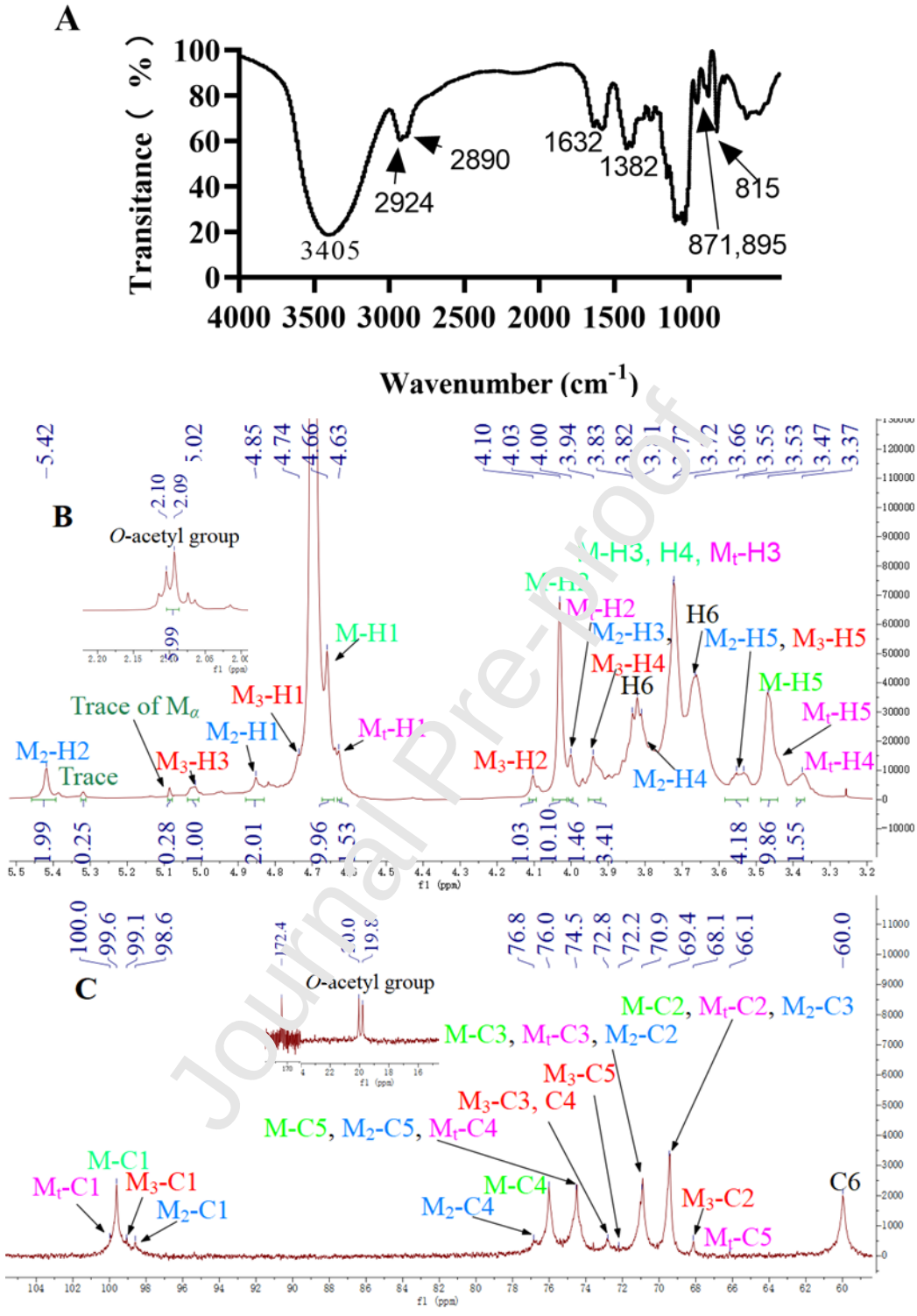

Fig.4. The FT-IR and 1D NMR spectra of DDP-1: (**A**) IR, (**B**) ^{1}H, (**C**) ^{13}C

3.4.2. Identification of residue M

The signals at 4.66 ppm in the ^{1}H NMR and 99.6 ppm in the ^{13}C NMR were unambiguously assigned to H-1 and C-1 of →4)-*β*-D-Man*p*-(1→ (designated M) according to literature

[23-25] and the results of methylation and monosaccharide composition. Moreover, considering the relatively high content of residue M, the strong signals 4.03, 3.82, 3.72, 3.66 and 3.47 in the ^{1}H NMR were assigned as the signals of residue M, which was further confirmed by the cross-peaks at 4.66 ppm/4.03 ppm, 4.66 ppm/3.82 ppm, 4.66 ppm/3.72 ppm, 4.66 ppm/3.66 ppm, and 4.66 ppm/3.47 in TOCSY spectrum (Fig. 5A and S9). Accordingly, the HSQC cross-signals at 3.82 ppm/60.0 ppm and 3.66 ppm/60.0 ppm were unambiguously ascribed as correlations of H-6/C-6 (Fig. 5B and S10). Once the chemical shift of H-6 was determined, the chemical shifts of H-5 and H-4 were easily obtained from the COSY correlations of H-5/H-6 (3.47 ppm/3.66 ppm) and H-4/H-5 (3.72 ppm/3.47 ppm) (Fig. 5C and S11). Based on the proton signals obtained, the H-1/C-1 (4.66 ppm/99.6 ppm), H-2/C-2 (4.03 ppm/69.4 ppm), H-3/C-3 (3.72 ppm/70.9 ppm), H-4/C-4 (3.72 ppm/76.0 ppm), H-5/C-5 (3.47 ppm/74.5 ppm), and H-6/C-6 (3.66 ppm/60.0 ppm, 3.82 ppm/60.0 ppm) cross-peaks of residue M were easily identified in the HSQC spectrum (Fig. 5B) and were listed in Table 2. These assignments of residue M were further supported by the HMBC correlations from H-1 (4.66 ppm) to C-2 (69.4 ppm); H-2 (4.03 ppm) to C-1 (99.6 ppm), C-3 (70.9 ppm), and C-4 (76.0 ppm); H-3 (3.72 ppm) to C-4 (76.0 ppm); H-4 (3.72 ppm) to C-3 (70.9 ppm) and C-6 (60.0 ppm); H-5 (3.47 ppm) to C-1 (99.6 ppm), C-3 (70.9 ppm), C-4 (76.0 ppm), and C-6 (60.0 ppm); H-6 (3.66 ppm) to C-4 (76.0 ppm) and C-5 (74.5 ppm) (Fig. 5D, E and S12).

3.4.3. Identification of residue M_2

The lowest-field signal at 5.42 ppm in at ^{1}H NMR was assigned to H-2 of →4)-2-*O*-acetyl-*β*-D-Man*p*-(1→ (designated M_2), based on literature data [24-26]. The other proton signals were observed by the TOCSY correlations between the H-2 (5.42 ppm) and each of H-1 (4.85 ppm), H-3 (3.94 ppm), H-4 (3.78 ppm), and H-5 (3.53 ppm) combined with the correlation of H-1(4.85 ppm)/H-6 (3.66 ppm) (Fig. 5A). This assignment was

further confirmed by the cross-signals of H-2/H-3 (5.42 ppm/3.94 ppm), H-3/H-4 (3.94 ppm/3.78 ppm), and H-4/H-5 (3.78

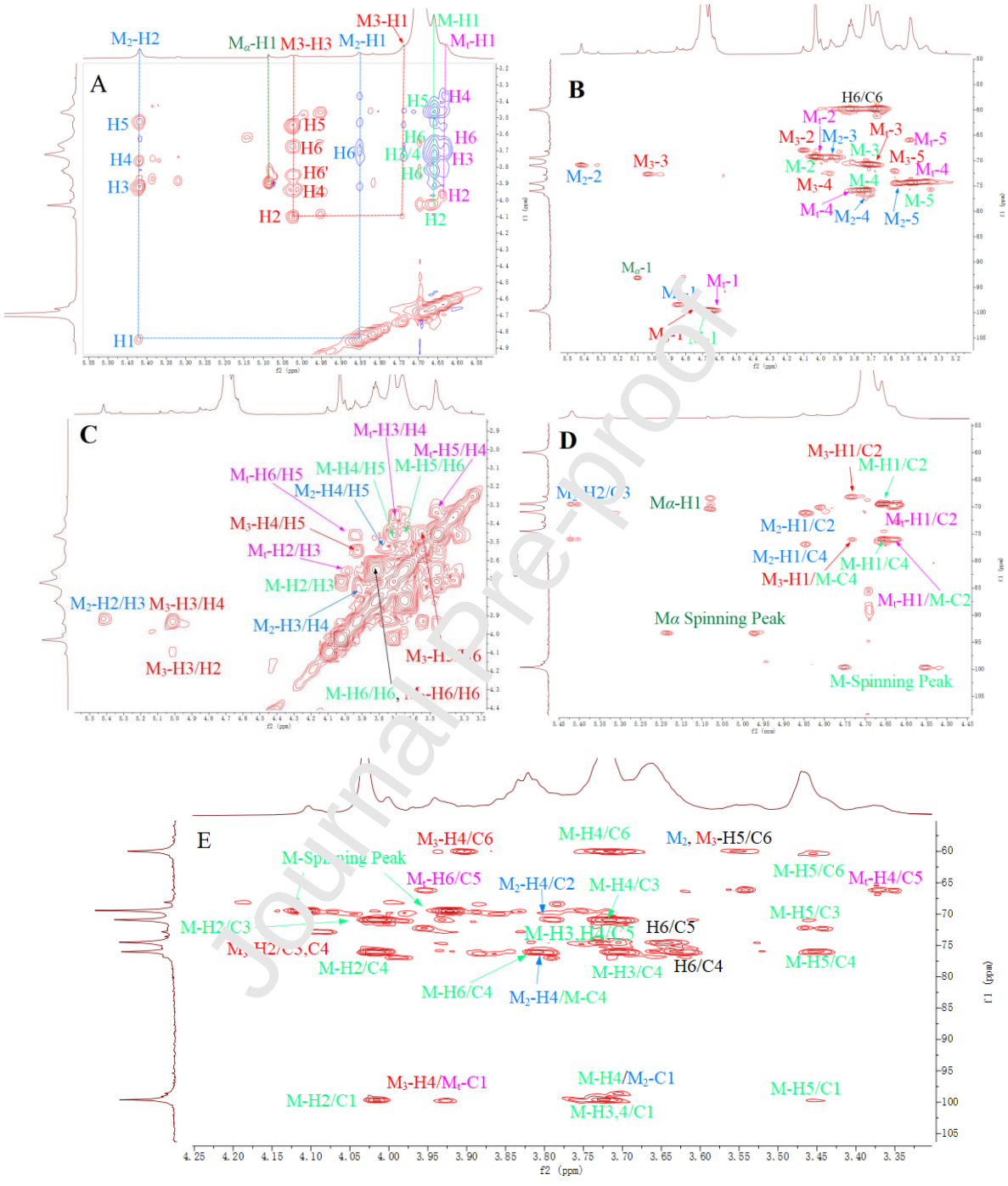

Fig.5. The 2D NMR spectra of DDP-1: (**A**) TOCSY, (**B**) HSQC, (**C**) COSY, (**D**, **E**) HMBC (**D** for region from 4.45 to 5.45 ppm, **E** for region from 3.33 to 4.25 ppm)

ppm/3.53 ppm) in the COSY spectrum (Fig. 5C). Once the ^{1}H chemical shifts assigned, the ^{13}C chemical shifts were obtained from the cross- peaks of H-1/C-1 (4.85 ppm/98.6 ppm),

H-2/C-2 (5.42 ppm/70.9 ppm), H-3/C-3 (3.94 ppm/69.4 ppm), H-4/C-4 (3.78 ppm/76.0 ppm), H-5/C-5 (3.53 ppm/74.5 ppm), and H-6/C-6 (3.66 ppm/60.0 ppm) in the HSQC spectrum (Fig. 5B). This interpretion was verified by HMBC correlations of H-1/C-2 (4.85 ppm/70.9 ppm), H-2/C-3 (5.42 ppm/69.4 ppm) and H-2/carbonyl carbon of *O*-acetyl groups (5.42 ppm/172.4 ppm), H-4/C-2 (3.78 ppm/70.9 ppm), H-5/C-6 (3.53 ppm/60.0 ppm), and H-6/C-5 (3.66 ppm/74.5 ppm) (Fig. 5D and E).

3.4.4. Identification of residue M_3

The presence of →4)-3-*O*-acetyl-*β*-D-Man*p*-(1→ (designated M_3) was revealed by its characteristic H-1 signals at 5.07 ppm, according to literature [24-26]. Accordingly, the ^{1}H NMR signals at 4.10 ppm, 3.94 ppm, and 3.55 were attributed to H-2, H-4, and H-5, respectively, based on the cross-peaks of H-3/H-2 (5.02 ppm/4.10 ppm), H-3/H-4 (5.02 ppm/3.94 ppm), H-4/H-5 (3.94 ppm/3.55 ppm) in the COSY spectrum (Fig. 5C), which was further supported by the cross-signals of H-3/H-2 (5.02 ppm/4.10 ppm), H-3/H-4 (5.02 ppm/3.94 ppm), H-3/H-5 (5.02 ppm/3.55 ppm) in the TOCSY spectrum (Fig. 5A). Once the proton chemical shifts of H-2, H-3, H-4 and H-5 determined, the corresponding carbon chemical shifts were assigned by HSQC correlations of H-2/C-2 (4.10 ppm/68.1 ppm), H-3/C-3 (5.02 ppm/72.8 ppm), H-4/C-4 (3.94 ppm/72.8 ppm), H-5/C-5 (3.55 ppm/72.2 ppm) (Fig. 5B). The chemical shifts of H-6 (3.66, 3.82 ppm) and C-6 (60.0 ppm) were easily assigned because of only one methylene group observed in all NMR spectra, combined with the HMBC correlations from H-4 (3.94 ppm) to C-6 (60.0 ppm) (Fig. 5E). The chemical shift of H-1 was assigned 4.74 ppm by the cross-signals of H-1 (4.74 ppm)/C-2 (68.1 ppm) in the HMBC spectrum and based on literature [27, 28] (Fig. 5D). The chemical shift of C-1 was assigned 99.1 ppm by the cross-signals of H-1 (4.74 ppm)/C-1 (99.1 ppm) in the HSQC spectrum (Fig. 5B).

3.4.5. Identification of residue M_t

The anomeric signals at 4.63 ppm and 100.0 ppm in the 1D NMR spectra and HSQC spectrum were assigned as H-1 and C-1 of non-reducing end *β*-D-Man*p*-(1→ (designated M_t) according

Table 2. The chemical shifts of DDP-1

	^{1}H and ^{13}C chemical shifts in ppm (δ_H/δ_C)					
Residue	1	2	3	4	5	6
M_t	4.63/100.0	3.99/69.4	3.70/70.9	3.37/74.5	3.46/66.1	3.66,3.93/60.0
M	4.66/99.6	4.03/69.4	3.72/70.9	3.72/76.0	3.47/74.5	3.66,3.82/60.0
M_2	4.85/98.6	5.42/70.9	3.94/69.4	3.78/76.8	3.53/74.5	3.66/60.0
M_3	4.74/99.1	4.10/68.1	5.02/72.8	3.94/72.8	3.55/72.2	3.66,3.82/60.0

M_t: Man*p*-(1→, M: →4)-Man*p*-(1→, M_2: →4)-2-*O*-acetyl-*β*-D-Man*p*-(1→, M_3: →4)-3-*O*-acetyl-*β*-D-Man*p*-(1→

to literature [27, 29].The other proton signals were observed by the TOCSY correlations between the H-1 (4.63 ppm) and each of H-2 (3.99 ppm), H-3 (3.70 ppm), H-4 (3.37 ppm), H-5 (3.46 ppm), and H-6 (3.66 ppm) as well as the cross-signals of H-2/H-3 (3.99 ppm/3.70 ppm), H-6/H-5 (3.93 ppm/3.46 ppm), H-3/H-4 (3.70 ppm/3.37 ppm), H-5/H-4 (3.46 ppm/3.34 ppm) in the COSY spectrum (Fig. 5B and C). Accordingly, the ^{13}C chemical shifts were assigned from the cross peaks of H-1/C-1 (4.63 ppm/100.0 ppm), H-2/C-2 (3.99 ppm/69.4 ppm), H-3/C-3 (3.70 ppm/70.9 ppm), H-4/C-4 (3.37 ppm/74.5 ppm), H-5/C-5 (3.46 ppm/66.1 ppm), and H-6/C-6 (3.66, 3.93 ppm/60.0 ppm) in the HSQC spectrum (Fig. 5B). These NMR data indicated that DDP-1 had M, M_2, M_3, and M_t residues, which was consistent with the results of methylation analysis (Table 1).

3.4.6. Glycosidic linkages of saccharide residues

The glycosidic linkages were identified by HMBC spectrum (Fig. 5D and E). The cross-peak of H-1(4.85 ppm)/C-4 (3.37 ppm/76.8 ppm) of residue M_2 in the HMBC spectrum showed the presence of -M_2-M_2- sequences. The anomeric proton (4.66 ppm) of residue M had the correlation with C-4 (76.8 ppm) of residue M_2 indicated the residue M was linked to C-4 of

residue M_2 (indicated the existence of -M-M_2-M_2- glycosidic linkages), which was further confirmed by the correlation between H-4 (3.78 ppm) of residue M_2 with C-4 (76.0 ppm) of residue M. The correlation of H-4 (3.72 ppm) of residue M with C-1 (98.1 ppm) of residue M_2 suggested that residue M_2 was linked to the C-4 of residue M (the existence of -M-M_2-M_2-M-). The cross-signals of H-1 (4.66 ppm)/C-4 (76.0 ppm) of residue M showed the -M-M- sequence. The cross-peaks at 4.74/76.0 (M_3-H1/M-C4) and 3.94/99.6 ppm (M_3-H4/M-C1) implied the linkage sequences of -M-M_3- and -M_3-M-. The cross-peak at 4.63/76.0 (M_t-H1/M-C4) indicated that the H-1 of residue M_t was linked to C-4 of residue M. By comparing the integration area of anomeric protons in M, M_2, M_3, and M_t, the ratio was 10:2:1:1. Thus the repeated unit of DDP-1 was inferred and showed in Fig. 6 with the aid of free software DrawGlycan-SNFG [30]. This result showed that the fine structure of DDP-1 varied from other *Dendrobium* polysaccharides [21].

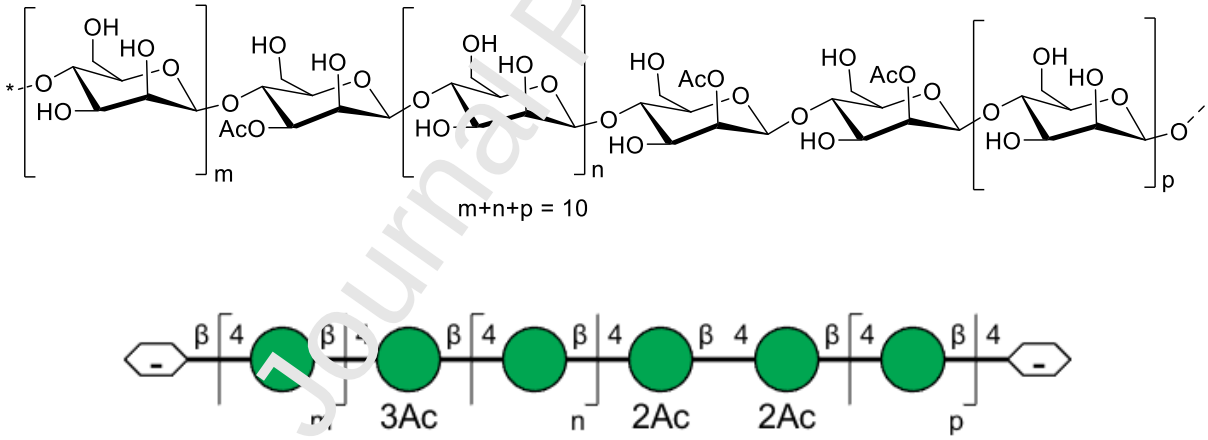

Fig. 6. Proposed structure of DDP-1

3.5. The effects of purification process on the microstructure of DDP-1

Acemannan has been widely used in biomedical materials, which was closely related with its microstructure [31, 32]. To explore the effects of purification process on microstructure of DDP-1, the images of samples at different purification process are shown in Fig. 7 (2.00 KX) and S13–25 (500 X, 10 KX and 100 KX). The crude polysaccharide displayed an irregular thin debris shape (Fig. 7A and S13–15). This chaotic structure might be result from the

effects of different materials on polysaccharide hydrogen-bond interaction due to the heterogeneity of crude polysaccharide. Ethanol precipitation revealed dense microalveoles with irregular size arranged in a honeycomb structure (Fig. 7B and S16–18), which was attribute to phase separation induced by the residual ethanol [33]. The SEM examination of other samples showed a mesh-like architecture (Fig. 7C–E and S18–25). On the whole, the surface of DDP-1 was compact and crosslinked whereas the samples purified from membrane filtration and DEAE52 had looser and less crosslinked appearance. The microstructure of DDP-1 facilitated its interactions with other substances, indicating it can be used in hydrophilic polymer materials [34].

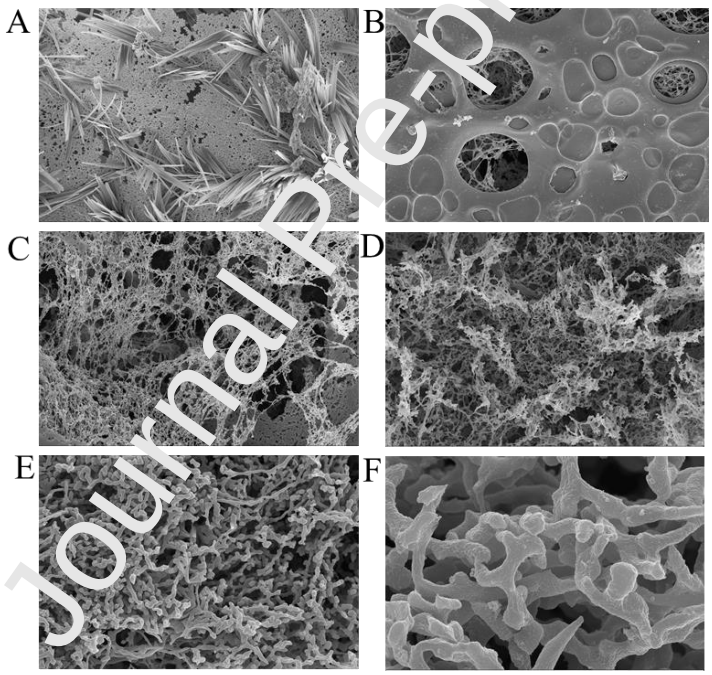

Fig. 7. Microstructure of samples. (**A**) Crude polysaccharides, (**B**) Ethanol precipitation, (**C**) Membrane filtration, (**D**) DEAE52, (**E, F**) DDP-1 (2 KX and 10 KX).

Biological evaluation of DDP-1

To discover the biological activity of DDP-1, the immunomodulatory and anticancer activities of DDP-1 were estimated *in vitro*. TNF-*α* and IL-6 are cytokines secreted mainly by macrophages and have been recognised widely as the important host-regulatory

molecules [35-37]. Therefore, immunostimulatory effects of DDP-1 were evaluated based on the production levels of these cytokines. Our results suggested that DDP-1 had the ability to enhance the production of TNF-α and IL-6 secreted by THP-1 macrophage cells. The titers of TNF-α stimulated by DDP-1 increased significantly in a dose and time dependent manner (Fig. 8A). The effects of DDP-1 on IL-6 content are different from TNF-α. The increased production of IL-6 was only observed at 6 h after DDP-1 treatment (Fig. 8B). In addition, DDP-1 showed slower and weaker immune response compared with LPS treatment, which presented DDP-1 has significant immune-modulating activity properties as an immune-stimulant. The difference between effects of DDP-1 and LPS on cytokines production was maybe involved in the diverse mechanisms of immune response to LPS and DDP-1, which needs further study.

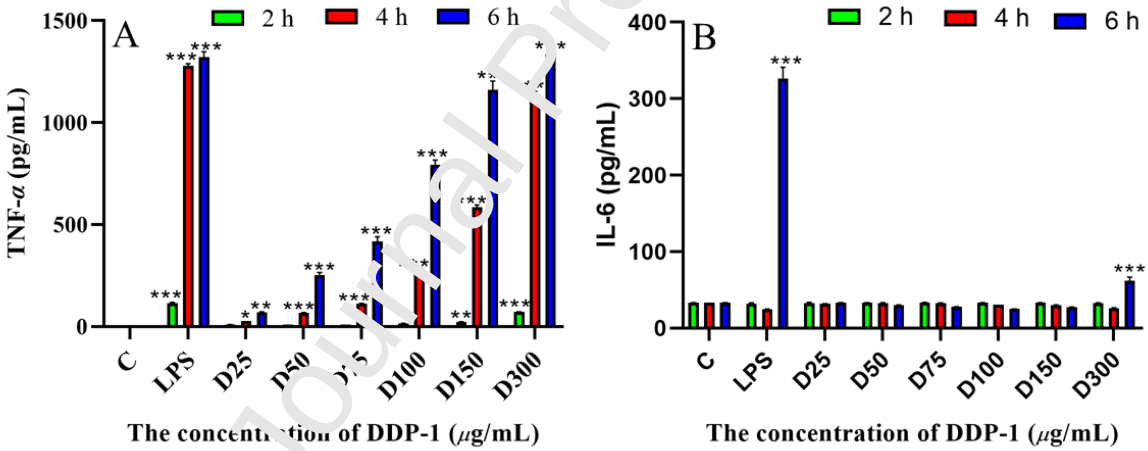

Fig. 8. Immunomodulatory effects of DDP-1. (**A**) TNF-α, (**B**) IL-6

The anticancer activities of DDP-1 were investigated at different concentrations (25, 50, 75, 100, 150, 300 μg/mL) on four tumor cell lines (HepG2, A431, H1975, MCF-7). The results demonstrate that the growth inhibition rates on HepG2 increased significantly in a dose-dependent manner with polysaccharide-treated cells, which was stronger than positive control (Fig. 9A). Furthermore, the growth inhibition to michigan cancer foundation-7, a woman breast cancer cell line (MCF-7), also increased along with the increased

concentration of DDP-1 (Fig. 9B). For A431, and H1975, DDP-1 treatment had no significant effects on cell viability compared with the effect of the control treatment on tumor cells at doses up to 100 μg/mL (Fig. 9C and D).

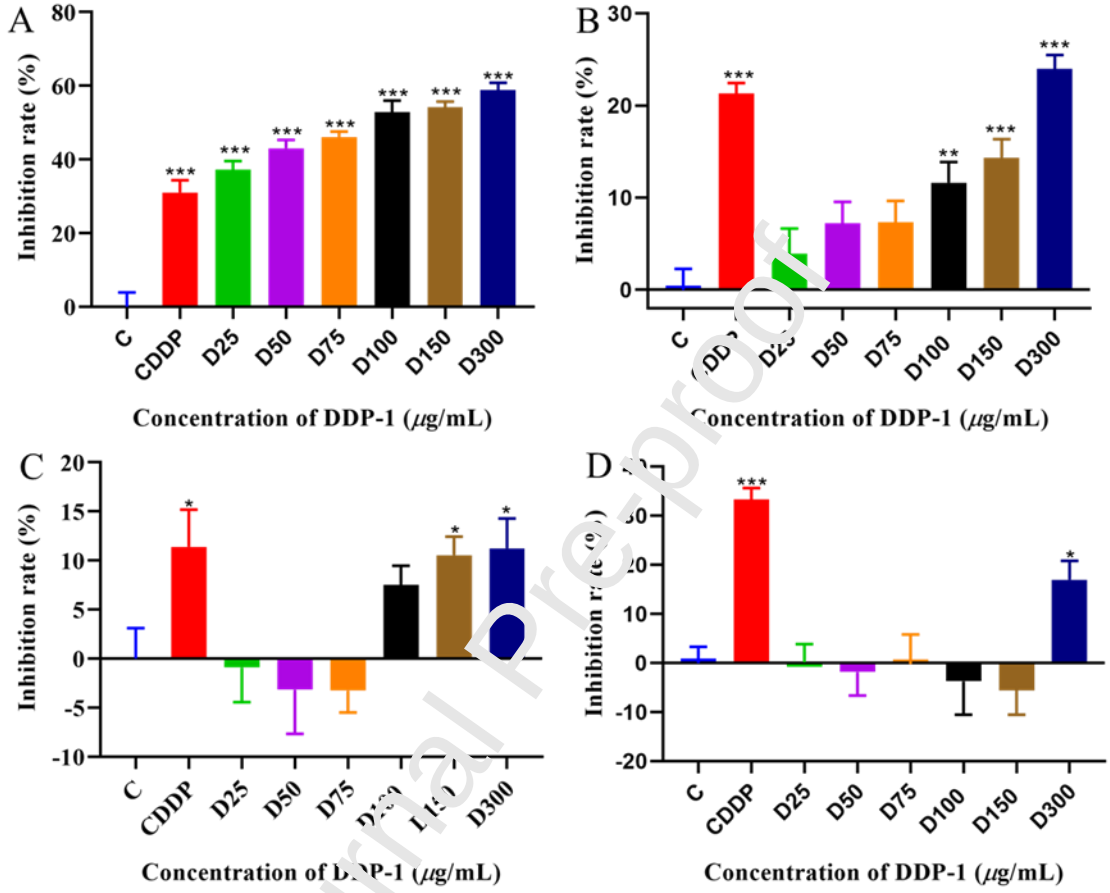

Fig. 9. Anticancer activities of DDP-1. (**A**) Human hepatoma cell line (HepG2). (**B**) Human breast cancer cell line (MCF-7). (**C**) Cutaneous squamous carcinoma cell line (A431). (**D**) Human non-small cell lung adenocarcinoma cell line (H1975).

4. Conclusions

To date, the related researches mainly focus on micromolecules and crude polysaccharides from this plant [21]. In this study, DDP-1, a leading water-soluble polysaccharide of *D. devonianum* stem, was isolated and identified to be a homopolysaccharide, (1→4)-*β*-D-acemannan, which varied from other *Dendrobium* species polysaccharides [21]. In addition, biological activity evaluation including immunomodulatory and antitumor

indicated it had positive effects against hepatoma and breast cancer cells as well as negative effect against human epidermoid carcinoma A431 and human lung adenocarcinoma 1975 cells besides possessing immunomodulatory activities. The information of this research and published literatures can tell that (1→4)-*β*-D-acetylated mannan is one of the key biomacomolecules for health beneficial functions and drug development of *D. devonianum*. Further work on the structure-activity relationship and mechanism of immunomodulatory and antitumor action of DDP-1 is worthy to be conducted. In consideration of the potential application of DDP-1 in materials, the research on application of DDP-1 in hydrogel is in progress.

ACKNOWLEDGEMENTS

Authors are thanking teachers in Analysis and Test Center of Kunming Institute of Botany for help with instrumental analysis. This work was funded by the National Natural Science Foundation of China (32170407), Biological Resources Programme, Chinese Academy of Sciences (KFJ-BRP-007-019) and Longling county.

REFERENCES

[1] Y.-G. Wu, K.-W. Wang, Z.-R. Zhao, P. Zhang, H. Liu, G.-J. Zhou, Y. Cheng, W.-J. Wu, Y.-H. Cai, B.-L. Wu, F.-Y. Chen, A novel polysaccharide from *Dendrobium devonianum* serves as a TLR4 agonist for activating macrophages, Int. J. Biol. Macromol. 133 (2019) 564-574. https://doi.org/10.1016/j.ijbiomac.2019.04.125.

[2] Y.-M. Xing, J. Chen, J.-L. Cui, X.-M. Chen, S.-X. Guo, Antimicrobial Activity and Biodiversity of Endophytic Fungi in *Dendrobium devonianum* and *Dendrobium thyrsiflorum* from Vietman, Curr. Microbiol. 62(4) (2010) 1218-1224. https://doi.org/10.1007/s00284-010-9848-2.

[3] L. Tong, L. Wang, X. Zhou, K. Zhong, L. Liu, F. Wang, S. Zhou, Antitumor activity of *Dendrobium devonianum* polysaccharides based on their immunomodulatory effects in S180 tumor-bearing mice, RSC Adv. 6(46) (2016) 40250-40257. https://doi.org/10.1039/C6RA03074B

[4] X.-Q. Zha, J.-P. Luo, S.-Z. Luo, S.-T. Jiang, Structure identification of a new immunostimulating polysaccharide from the stems of *Dendrobium huoshanense*, Carbohydr. Polym. 69(1) (2007) 86-93. https://doi.org/10.1016/j.carbpol.2006.09.005.

[5] J.-H. Wang, J.-P. Luo, X.-F. Yang, X.-Q. Zha, Structural analysis of a rhamnoarabinogalactan from the stems of *Dendrobium nobile Lindl*, Food Chem. 122(3) (2010) 572-576. https://doi.org/10.1016/j.foodchem.2010.03.012.

[6] J.-H. Wang, J.-P. Luo, X.-Q. Zha, B.-J. Feng, Comparison of antitumor activities of different polysaccharide fractions from the stems of *Dendrobium nobile Lindl*, Carbohydr. Polym. 79(1) (2010) 114-118. https://doi.org/10.1016/j.carbpol.2009.07.032.

[7] A. Luo, X. He, S. Zhou, Y. Fan, A. Luo, Z. Chun, Purification, composition analysis and antioxidant activity of the polysaccharides from *Dendrobium nobile Lindl*, Carbohydr. Polym. 79(4) (2010) 1014-1019. https://doi.org/10.1016/j.carbpol.2009.10.033.

[8] K. Zhang, X. Zhou, J. Wang, Y. Zhou, W. Qi, H. Chen, S. Nie, M. Xie, *Dendrobium officinale* polysaccharide triggers mitochondrial disorder to induce colon cancer cell death via ROS-AMPK-autophagy pathway, Carbohydr. Polym. 264 (2021) 118018. https://doi.org/10.1016/j.carbpol.2021.118018.

[9] Y.-P. Huang, T.-B. He, X.-D. Cuan, X.-J. Wang, J.-M. Hu, J. Sheng, 1,4-*β*-D-glucomannan from *Dendrobium officinale* activates NF-*κ*B via TLR4 to regulate the immune response, Molecules 23(10) (2018) 2658. https://doi.org/10.3390/molecules23102658.

[10] M.-T. Kuang, J.-Y. Li, X.-B. Yang, L. Yang, J.-Y. Xu, S. Yan, Y.-F. Lv, F.-C. Ren, J.-M. Hu, J. Zhou, Structural characterization and hypoglycemic effect via stimulating glucagon-like peptide-1 secretion of two polysaccharides from *Dendrobium officinale*, Carbohydr. Polym. 241 (2020) 116326. https://doi.org/10.1016/j.carbpol.2020.116326.

[11] T.-B. He, Y.-P. Huang, L. Yang, Y.-T. Liu, W.-Y. Gong, X.-J. Wang, J. Sheng, J.-M. Hu, Structural characterization and immunomodulating activity of polysaccharide from *Dendrobium officinale*, Int. J. Biol. Macromol. 83 (2016) 34-41. https://doi.org/10.1016/j.ijbiomac.2015.11.038.

[12] Y. Deng, M. Li, L.-X. Chen, X.-Q. Chen, J.-H. Lu, J. Zhao, S.-P. Li, Chemical characterization and immunomodulatory activity of acetylated polysaccharides from *Dendrobium devonianum*, Carbohydr. Polym. 180 (2018) 238-245. https://doi.org/10.1016/j.carbpol.2017.10.026.

[13] D. Wang, B. Fan, Y. Wang, L. Zhang, F. Wang, Optimum extraction, characterization, and antioxidant activities of polysaccharides from flowers of *Dendrobium devonianum*, Int. J. Anal. Chem. 2018 (2018) 3013497. https://doi.org/10.1155/2018/3013497.

[14] Z. Zhang, D. Li, X. Li, Z. Guo, Y. Liu, X. Ma, S. Zheng, PEI-modified macrophage cell membrane-coated PLGA nanoparticles encapsulating *Dendrobium* polysaccharides as a

vaccine delivery system for ovalbumin to improve immune responses, Int. J. Biol. Macromol. 165 (2020) 239-248. https://doi.org/10.1016/j.ijbiomac.2020.09.187.

[15] J.-J. Cao, Q.-Q. Lv, B. Zhang, H.-Q. Chen, Structural characterization and hepatoprotective activities of polysaccharides from the leaves of *Toona sinensis* (A. Juss) *roem*, Carbohydr. Polym. 212 (2019) 89-101. https://doi.org/10.1016/j.carbpol.2019.02.031.

[16] Y. Feng, I.C. Juliet, C. Wen, Y. Duan, J. Zhou, Y. He, H. Zhang, H. Ma, Effects of multi-mode divergent ultrasound pretreatment on the physicochemical and functional properties of polysaccharides from *Sagittaria sagittifolia* L, Food Biosci. 42 (2021) 101145. https://doi.org/10.1016/j.fbio.2021.101145.

[17] M.G. Sevag, D.B. Lackman, J. Smolens, The isolation of the components of streptococcal nucleoproteins in serologically active form, J. Biol. Chem. 124 (1938) 425-436. https://doi.org/10.1016/S0021-9258(18)74048-9.

[18] M. Dubois, K. Gilles, J.K. Hamilton, P.A. Rebers, F. Smith, A colorimetric method for the determination of sugars, Nature 168(4265) (1951) 167-167. https://doi.org/10.1038/168167a0.

[19] A.A. Herod, K.D. Bartle, R.J. Morgan, R. Kandiyoti, Analytical methods for characterizing high-mass complex polydisperse hydrocarbon mixtures: an overview, Chem. Rev. 112(7) (2012) 3892-923. https://doi.org/10.1021/cr200429v.

[20] V.P. Kodali, R.S. Perali, R. Sen, Purification and partial elucidation of the structure of an antioxidant carbohydrate biopolymer from the probiotic bacterium *Bacillus coagulans* RK-02, J. Nat. Prod. 74(8) (2011) 1692-1697. https://doi.org/10.1021/np1008448.

[21] H. Yue, H. Zeng, K. Ding, A review of isolation methods, structure features and bioactivities of polysaccharides from Dendrobium species, Chin. J. Nat. Med. 18(1) (2020) 1-27. https://doi.org/10.1016/S1875-5364(20)30001-7.

[22] S.M. Hoseiniyan Benvidi, K. Jahanbin, A new water-soluble polysaccharide from *Echinops pungens* Trautv roots. Part I. Isolation, purification, characterization and antioxidant activity, Int. J. Biol. Macromol. 161 (2020) 909-916. https://doi.org/10.1016/j.ijbiomac.2020.06.128.

[23] Z.K. Muhidinov, J.T. Bobokalonov, I.B. Ismoilov, G.D. Strahan, H.K. Chau, A.T. Hotchkiss, L. Liu, Characterization of two types of polysaccharides from *Eremurus hissaricus* roots growing in Tajikistan, Food Hydrocolloids 105 (2020) 105768. https://doi.org/10.1016/j.foodhyd.2020.105768.

[24] Y.-f. Hua, M. Zhang, C.-x. Fu, Z.-h. Chen, G.Y.S. Chan, Structural characterization of a 2-*O*-acetylglucomannan from *Dendrobium officinale* stem, Carbohydr. Res. 339(13) (2004) 2219-2224. https://doi.org/10.1016/j.carres.2004.05.034.

[25] X. Zhang, C. Bi, H. Shi, X. Li, Structural studies of a mannoglucan from *Cremastra appendiculata* (Orchidaceae) by chemical and enzymatic methods, Carbohydr. Polym. 272 (2021) 118524. https://doi.org/10.1016/j.carbpol.2021.118524.

[26] X. Xing, S.W. Cui, S. Nie, G.O. Phillips, H.D. Goff, Q. Wang, Study on *Dendrobium officinale O*-acetyl-glucomannan (Dendronan®): Part II. Fine structures of *O*-acetylated residues, Carbohydr. Polym. 117 (2015) 422-433. https://doi.org/10.1016/j.carbpol.2014.08.121.

[27] T. Hannuksela, C. Hervé du Penhoat, NMR structural determination of dissolved *O*-acetylated galactoglucomannan isolated from spruce thermomechanical pulp, Carbohydr. Res. 339(2) (2004) 301-312. doi.org/10.1016/j.carres.2003.10.025.

[28] J. Lundqvist, A. Teleman, L. Junel, G. Zacchi, O. Dahlman, F. Tjerneld, H. Stålbrand, Isolation and characterization of galactoglucomannan from *spruce* (Picea abies), Carbohydr. Polym. 48(1) (2002) 29-39. https://doi.org/10.1016/S0144-8617(01)00210-7.

[29] R. Goldberg, L. Gillou, R. Prat, C.H. Du Penhoat, V. Michon, Structural features of the cell-wall polysaccharides of *Asparagus officinalis* seeds, Carbohydr. Res. 210 (1991) 263-276. https://doi.org/10.1016/0008-6215(91)80128-A.

[30] K. Cheng, Y. Zhou, S. Neelamegham, DrawGlycan-SNFG: a robust tool to render glycans and glycopeptides with fragmentation information, Glycobiology 27(3) (2016) 200-205. https://doi.org/10.1093/glycob/cww115.

[31] H. Baniasadi, R. Ajdary, J. Trifol, O.J. Rojas, J. Seppälä, Direct ink writing of aloe vera/cellulose nanofibrils bio-hydrogels, Carbohydr. Polym. 266 (2021) 118114. https://doi.org/10.1016/j.carbpol.2021.118114.

[32] D.I. Sánchez-Machado, J. López-Cervantes, R. Sendón, A. Sanches-Silva, *Aloe vera*: Ancient knowledge with new frontiers, Trends Food Sci. Technol. 61 (2017) 94-102. https://doi.org/10.1016/j.tifs.2016.12.005.

[33] E. Dumay, A. Laligant, D. Zasypkin, J.C. Cheftel, Pressure- and heat-induced gelation of mixed *β*-lactoglobulin/polysaccharide solutions: scanning electron microscopy of gels, Food Hydrocolloids 13(4) (1999) 339-351. https://doi.org/10.1016/S0268-005X(99)00016-8.

[34] C. Chen, P. Zhou, C. Huang, R. Zeng, L. Yang, Z. Han, Y. Qu, C. Zhang, Photothermal-promoted multifunctional dual network polysaccharide hydrogel adhesive for infected and susceptible wound healing, Carbohydr. Polym. 273 (2021) 118557. https://doi.org/10.1016/j.carbpol.2021.118557.

[35] S. Bourcier, A. Sansonetti, L. Durand, C. Chomienne, J. Robert-Lezenes, F. Smadja-Joffe, CD44-ligation induces, through ERK1/2 pathway, synthesis of cytokines TNF-*α* and IL-6 required for differentiation of THP-1 monoblastic leukemia cells, Leukemia 24(7) (2010) 1372-5. https://doi.org/10.1038/leu.2010.100.

[36] C.S. Shi, K. Shenderov, N.N. Huang, J. Kabat, M. Abu-Asab, K.A. Fitzgerald, A. Sher, J.H. Kehrl, Activation of autophagy by inflammatory signals limits IL-1*β* production by

targeting ubiquitinated inflammasomes for destruction, Nat. Immunol. 13(3) (2012) 255-63. https://doi.org/10.1038/ni.2215.

[37] X. Xu, J. Li, Y. Hu, Polysaccharides from *Inonotus obliquus* sclerotia and cultured mycelia stimulate cytokine production of human peripheral blood mononuclear cells in *vitro* and their chemical characterization, Int. Immunopharmacol. 21(2) (2014) 269-78. https://doi.org/10.1016/j.intimp.2014.05.015.

CRediT authorship contribution statement

Tao-Bin He, Methodology, Investigation, Data curation, Writing. Yan-Ping Huang, Formal analysis, Investigation, Data curation. Xuan-Jun Wang, Validation, Data curation. Jun Sheng, Data curation, Resources, Validation. Jiang-Miao Hu: Conceptualization, Formal analysis, Writing - review & editing, Supervision, Project administration, Funding acquisition.

Graphical abstract for

Structural characterization and biological evaluation of an key *O*-acetyl-1,4-linked-*β*-D-mannan from *Dendrobium devonianum*

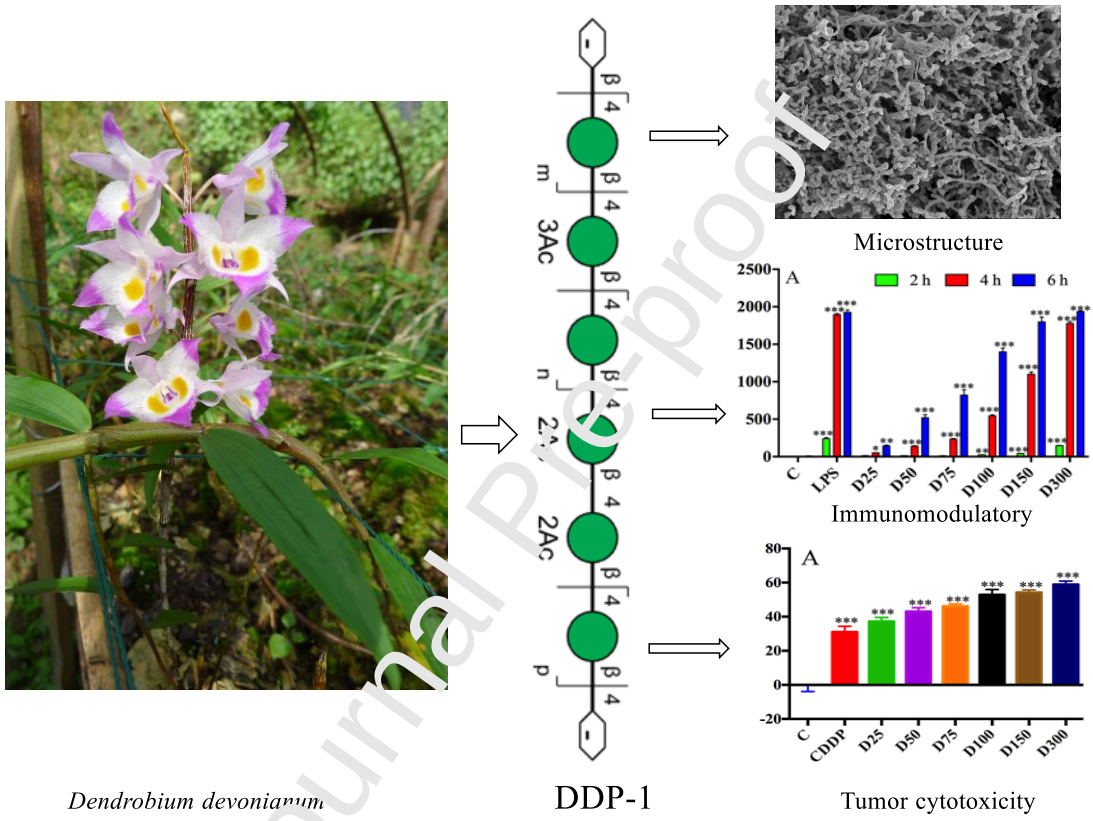

Highlights

(1) The fine structure of *Dendrobium devonianum* polysaccharide was firstly elucidated.

(2) Anticancer assay in vitro revealed that DDP-1 had cytotoxic activity against the growth of HepG2 and MCF-7 cancer cells.

(3) DDP-1 presented remarkable immune-enhancing properties in vitro.

(4) The microstructure features of DDP-1 indicated that DDP-1 hold high potential application in hydrophilic polymer materials.